Effect of molecular architectures in photoinduced birefringence in films of azo-modified diblock copolymers

Luciana M. Sáiz [a], Ileana A. Zucchi [a], Patricia A. Oyanguren [a], María J. Galante [a,*], Rafaela C. Sanfelice [b], Debora T. Balogh [b], Osvaldo N. Oliveira Jr. [b]

[a] Grupo de Polímeros Nanoestructurados, Instituto de Investigaciones en Ciencia y Tecnología de Materiales (INTEMA), Universidad Nacional de Mar del Plata, Consejo Nacional de Investigaciones Científicas y Técnicas (CONICET), J.B. Justo 4302, 7600 Mar del Plata, Argentina
[b] São Carlos Institute of Physics, University of São Paulo, CP 369, 13560-970 São Carlos, SP, Brazil

ABSTRACT

Langmuir films of polystyrene-block-poly(4-vinylpyridine) (PS-*b*-P4VP) with an azo dye, 4-[4-(phenylazo)-1-naphthylazo]phenol (Disperse Orange 13, DO13), hydrogen-bonded to the pyridine group of P4VP blocks were investigated. The surface pressure isotherms were considerably different for the copolymer dissolved in a nonselective (chloroform) and selective (toluene) solvents. The Langmuir–Blodgett (LB) and Langmuir–Schaefer (LS) films produced with PS-*b*-P4VP(DO13) copolymers displayed higher optically induced birefringence than the cast films owing to their nanostructured nature. The photoinduced birefringence properties were particularly enhanced when toluene was used owing to the confinement of azo chromophores in micelles consisting of a P4VP core and a PS corona.

© 2014 Published by Elsevier B.V.

1. Introduction

The control of molecular architectures has been a key ingredient for developing novel materials with enhanced properties for a variety of applications [1,2], and this can be achieved with techniques such as the Langmuir–Blodgett (LB) and the layer-by-layer (LbL) techniques [3–5]. LB films are produced by transferring Langmuir films from the air/water interface onto solid substrates by vertical dipping. The films may be highly organized because the molecules can be arranged in a controlled manner at the air–water interface, which allows one to fabricate well-defined structures, with controllable thickness and architecture. In cases where multilayer deposition with vertical dipping is not successful, use can be made of the Langmuir–Schaefer (LS) technique, a variant of the LB method where the film transfer is made horizontally [6]. Among the various types of properties for which the importance of molecular architecture has been demonstrated is the optical storage capability of films containing azobenzene compounds. [7–9]. Indeed, several molecular engineering strategies have been used to optimize both order and film thickness of this kind of materials.

The most important parameters for an efficient optical storage based on photoinduced birefringence are associated with the ability of the chromophores to be oriented and have this orientation preserved for long periods of time. These parameters depend on the intermolecular forces involving the chromophores and the free volume required for chromophore isomerization and reorientation [10]. The concept of free volume has been used to explain the photoisomerization process in LB films, which is based on the fact that trans-to-cis isomerization gives rise to increased cross-sectional area of the azobenzene. If the two dimensional structures of the LB films are preserved during photoisomerization, the sum of the cross-sectional areas of the molecules in any plane parallel to the substrate surface should not exceed the total film area of the as–deposited LB films. Hence, free volume should be necessary for photoisomerization in the LB films when the cross-section of the molecule increases during the process. When there is enough free volume, photoisomerization will proceed. On the other hand, if the molecules are closely packed in the film, the molecules will not photoisomerize [11].

Tuning the free volume and intermolecular interactions may be performed upon combining distinct materials in the films or by changing the properties of the polymers containing the azo chromophores. One such possibility is to produce micelles or aggregates from block copolymers in selective solvents for one of the blocks. The micelles are stabilized in solution via interactions of the soluble blocks with the solvent molecules [12]. Self-assembly of amphiphilic block copolymers at the air–water interface has been widely studied as an interesting route to generate distinct

* Corresponding author.
  E-mail address: galant@fi.mdp.edu.ar (M.J. Galante).

morphologies that can be transferred to solid substrates by LB or LS techniques [13–15]. In Langmuir films, if the corona-forming block of the solution micelles is attractive to water then the surface aggregation behavior may be a simple deposition of the micelles formed in the spreading solution. On the other hand, if the core-forming block of the solution micelles is attractive to water, then the block would tend to stretch on the water surface but the aggregates retained from the spreading solution would hinder the stretch [16]. In a previous work, we encapsulated a phenol-functionalized chromophore (Disperse Orange 13, DO13) within poly(styrene-*b*-4-vinylpyridine) (PS-*b*-P4VP) micelles in toluene by means of H-bond interactions between the phenol group of DO13 molecules and pyridine groups of P4VP block. DO13 was used as building block of micellar aggregates to manipulate the morphology, which allowed birefringence to be induced in spin-coated films produced with the micellar solutions [17].

In this paper we did the investigation by manipulating the morphology of LB, LS and spin-coated films using a selective and a non-selective solvents for the diblock copolymers. We shall show that the optical storage capability is enhanced when cooperative effects are exploited which depend on the confinement of azo chromophores in micelles. Before proceeding to the photoinduced birefringence experiments, a systematic study was performed of the effect from the solvent on the Langmuir film properties of the diblock copolymer.

2. Experimental section

2.1. Materials

A commercial symmetric diblock copolymer polystyrene-*b*-poly(4-vinylpyridine) (PS-*b*-P4VP) (MnPS = 22,000, MnP4VP = 22,000, Mw/Mn = 1.15) was purchased from Polymer Source, Inc. and used without further purification. The homopolymers poly-4-vinylpyridine (P4VP, Mn = 19,000, PDI = 1.15) and polystyrene (PS, Mn = 20,800, PDI = 1.07) were also purchased from Polymer Source, Inc. The selected chromophore was a push–pull diazo dye, 4-[4-(phenylazo)-1-naphthylazo]phenol (Disperse Orange 13, DO13, Aldrich). The chemical structures of DO13 and the block copolymer are shown in Fig. 1.

Chloroform (HPLC grade, ⩾99.8%; Sigma–Aldrich) and toluene (pro-analysis grade 99.5%, Biopack) were used for preparing the solutions. Ultrapure water with resistivity of 18.2 MΩ cm was obtained by purification of distilled water with a Millipore Milli-Q Gradient system and used as the subphase in the Langmuir trough.

2.2. Samples preparation

P4VP(DO13) supramolecules were prepared by dissolving P4VP and 25 or 40 wt.% of DO13 in chloroform. The solution was kept under stirring overnight to ensure H-bond formation between

Fig. 1. Chemical structures of PS-*b*-P4VP and DO13.

pyridine groups of P4VP and phenol groups of DO13. A slight heating (no more than 50 °C) of the solutions was required to ensure complete dissolution of both components. PS(DO13) solutions were prepared by dissolving PS and 25 or 40 wt.% of DO13 in chloroform. PS-*b*-P4VP(DO13) solutions were also obtained from chloroform (non selective solvent) and toluene (selective solvent for the PS block). First, PS-*b*-P4VP and 25 or 40 wt.% of DO13 were dissolved in chloroform and the procedure described above was followed again (step A in Fig. 2). The degree of complexation *r* (number of DO13 molecules per vinylpyridine repeating unit) of these samples was 0.2 and 0.4, respectively. To obtain the toluene solutions, chloroform was evaporated and toluene was added to the residue in order to form homogeneous micellar solutions. Sonication during 30 min followed by stirring was necessary to achieve complete dissolution of the residue. Micelles with a P4VP core containing the azo dye and a PS corona were developed (step B in Fig. 2), since toluene is a selective solvent for PS. Because toluene is not a good solvent for DO13, if some chromophore molecules were not attached to the core of the micelles, an orange precipitate would be observed. However, this was not the case here, at least in the range of degree of complexation explored (⩽1).

2.3. Fabrication of spin-coated films (SC)

Thin films were prepared from all solutions mentioned above by spin-coating onto cleaned glass substrates at 3000 rpm for 1 min. Glass substrates were previously cleaned with acetone, followed by sonication with isopropanol for 30 min, and finally dried under a stream of nitrogen gas. The resulting films were dried in vacuum for 24 h to remove residual solvent, and were ca. 40 nm thick for 3 wt.% solutions.

2.4. Fabrication of Langmuir Blodgett (LB) and Langmuir–Schaefer (LS) films

Films were prepared in a KSV 5000 trough, using spreading solutions with a typical concentration of 0.2 mg mL^{-1}. All the isotherms were measured inside a class 10,000 clean room, with the temperature controlled at 22 °C (room temperature). After solvent evaporation the Langmuir films were compressed at a barrier speed of 20 mm min^{-1}. Surface pressure–area (π–A) isotherms were measured using a Wilhelmy plate made of filter paper and the curve was computer-recorded. The mean molecular area values were calculated based on an average molecular weight obtained from the composition ratio of each component in the mixture. Main values of collapse pressure and zero pressure areas of solutions in chloroform and toluene of PS-*b*-P4VP and PS-*b*-P4VP(DO13), with 25 and 40 wt.% DO13 appear in Table 1.

The Langmuir films were transferred onto previously cleaned glass substrates in the form of LB and LS film at a surface pressure of 25–35 mN m^{-1} after waiting for 5 min for barrier stabilization. LB films were transferred onto glass substrates during vertical withdrawal from the subphase at a rate of 2 mm min^{-1}. The film thickness was determined by profilometry using a KLA Tencor D100 equipment, being the order of 10–30 nm.

2.5. Optical measurements

Photo-orientation experiments were carried out at room temperature and under ambient conditions, each time on a spot that had not been previously irradiated to avoid influence from irradiation history. The optical configuration for the measurement of photoinduced birefringence was similar to that in Ref. [18]. Photoinduced birefringence was measured by placing the film between two crossed linear polarizers. A semiconductor laser at 488 nm
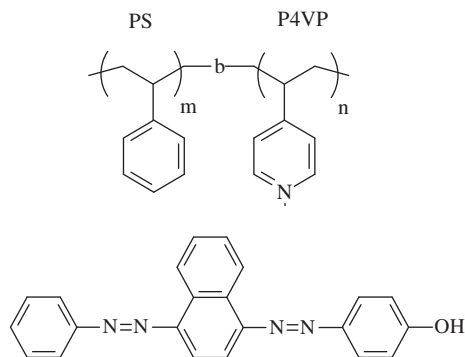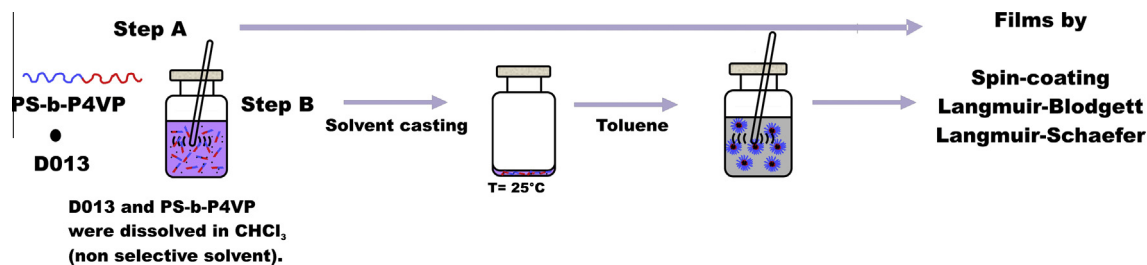
Fig. 2. Scheme for film preparation.

Table 1
Collapse pressure and zero pressure areas of solutions in chloroform and toluene of PS-*b*-P4VP and PS-*b*-P4VP(DO13) with 25 and 40 wt.% DO13.

Sample	Collapse pressure (mN m^{-1})	Zero pressure areas (A^2 molecule^{-1})
PS-*b*-P4VP (CHLO)	37	6.21
PS-*b*-P4VP(DO13)$_{25\%}$ (CHLO)	43	12.64
PS-*b*-P4VP(DO13)$_{40\%}$ (CHLO)	49	13.89
PS-*b*-P4VP (TOL)	66	4.97
PS-*b*-P4VP(DO13)$_{25\%}$ (TOL)	48	9.29
PS-*b*-P4VP(DO13)$_{40\%}$ (TOL)	53	12.66

was used as writing beam to induce optical anisotropy in the film, and a low-power semiconductor laser (5 mW) at 635 nm was used as reading beam to measure the light transmitted through the sample. To achieve maximum signal, the polarization vector of the writing beam was set to 45° with respect to the polarization vector of the reading beam. All the films were irradiated with 6 mW mm^{-2} of the writing laser in a 0.785 mm^2 spot. As a way of signing the UV–visible spectrum of DO13 is plotted in Fig. 3, indicating the position of both semiconductor lasers with respect to the absorption maximum.

The induced birefringence, Δn, was determined by measuring the probe beam transmission ($T = I/I_0$) according to:

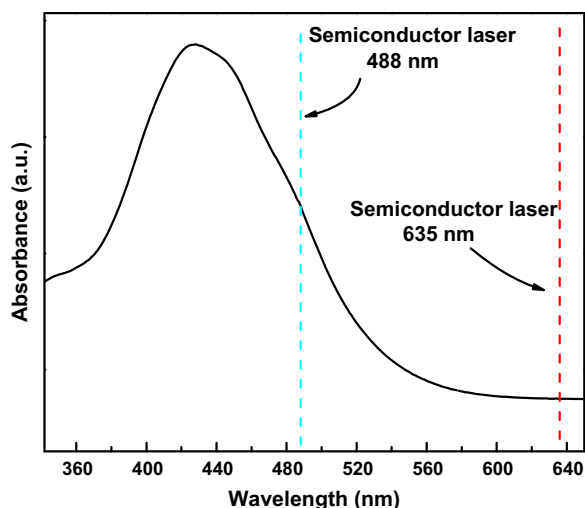$$\Delta n = (\lambda/\pi d)\sin^{-1}(I/I_0)^{1/2} \qquad (1)$$

Fig. 3. UV–visible spectrum of DO13.

where λ is the wavelength of the writing beam, d is the film thickness, I is the intensity after the second polarizer, and I_0 is the transmitted intensity between parallel polarizers, in absence of anisotropy.

3. Results and discussion

3.1. Effect of spreading solvents on isotherms

3.1.1. Non-selective solvent (chloroform)

Langmuir films of PS-*b*-P4VP and PS-*b*-P4VP(DO13), all dissolved in chloroform, were stable at the air/water interface, displaying the surface pressure (π–A) isotherms of Fig. 4. The isotherm of the pure copolymer exhibits a plateau-like region, typical of phase transitions such as the liquid-expanded to liquid-condensed transition. This part of the curve is associated with the P4VP block of the copolymer, inferred from the surface pressure isotherm for the homopolymers in Fig. 5a. The extrapolated area to zero pressure for the condensed phase of the monolayer was 6.2 A^2, which is approximately the area occupied by the repeating unit of the copolymer. For a series of diblock copolymers with the same PS block length and different P4VP lengths, Wen et al. [16] obtained larger areas per molecule for the copolymers with longer P4VP block.

The isotherms of the PS-*b*-P4VP(DO13) systems are shifted to larger areas per molecule due to the DO13 group that increases the area occupied by the repeating unit of the copolymer. In addition, for PS-*b*-P4VP(DO13) 40 wt.% the plateau region associated with the P4VP block disappears, which is evidence of H-bonding between DO13 and the pyridine group of P4VP. The areas extrapolated to zero pressure for DO13-containing copolymers were 12.6 and 13.9 A^2 for 25 and 40 wt.% DO13, respectively. The collapse pressure increased as more DO13 was attached to the sample, from 37 mN m^{-1} for the pure copolymer to 49 mN m^{-1} for the sample with 40 wt.% DO13.

3.1.2. Selective solvent (toluene)

The effect from the spreading solvent was studied by obtaining isotherms for the pure PS-*b*-P4VP spread with chloroform (non-selective solvent) and toluene (selective solvent). Fig. 6 shows that for toluene the plateau almost vanishes probably due to the use of a selective solvent for the PS block. Block copolymers in a selective solvent for one of the blocks are known to form micelles or aggregates as a result of the association of the insoluble blocks [19–22]. In our case, micelles with a P4VP core and a PS corona are formed as shown in a previous work [17]. Micellar size is the order of 40–50 nm. Owing to strong attraction, P4VP blocks tended to spread on the water surface when the solution micelles came into contact with the water. PS blocks tended to leave the water surface because they were incompatible with water and P4VP blocks. However, the aggregates retained from the spreading solution would hinder the stretch (or movement) of P4VP blocks on the water surface. Therefore, there are less surface-adsorbed P4VP
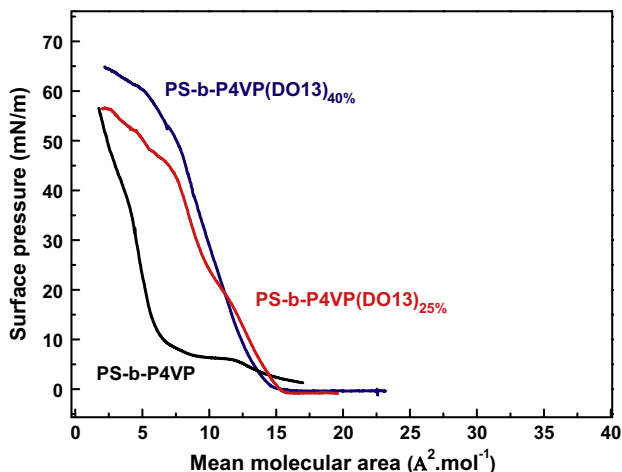
Fig. 4. Surface pressure isotherms of solutions in chloroform of PS-*b*-P4VP and PS-*b*-P4VP(DO13) with 25 and 40 wt.% DO13.
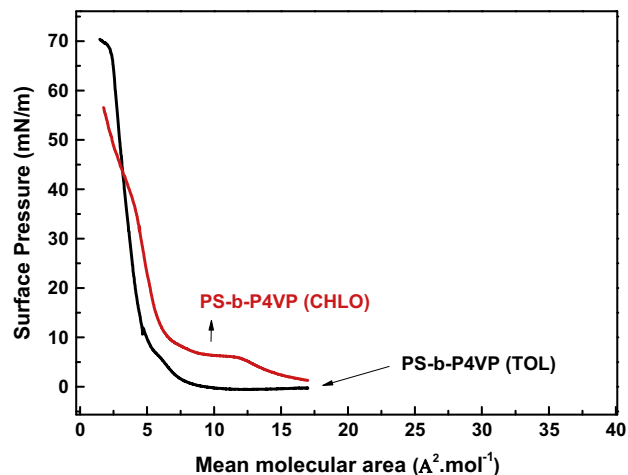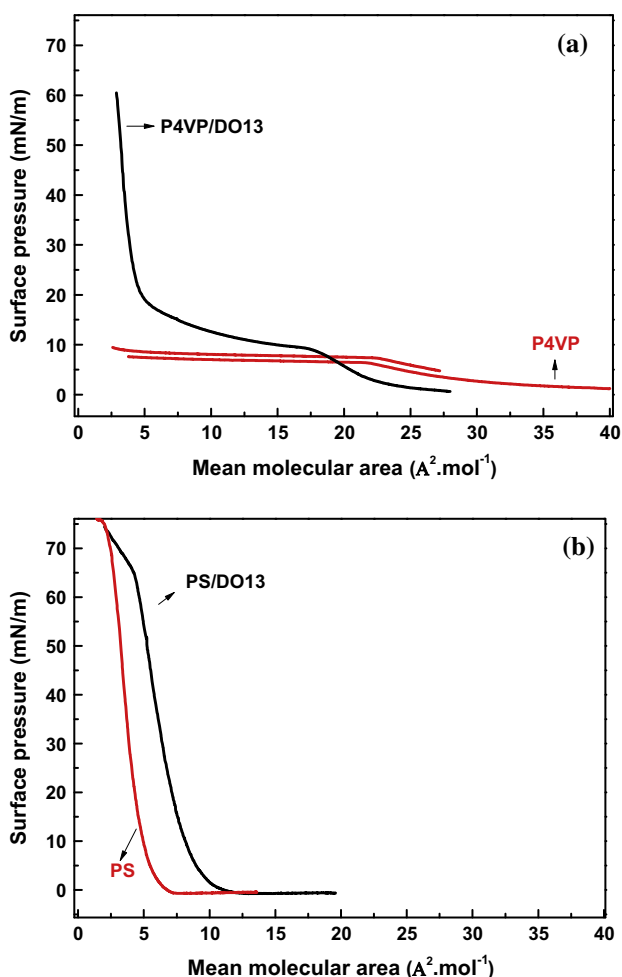

Fig. 5. Surface pressure isotherms for the homopolymers: (a) P4VP and P4VP(DO13) with 25 wt.% DO13 and (b) PS and PS(DO13) with 25 wt.% DO13.

blocks spread with toluene than those spread with chloroform [16]. Moreover, the collapse pressure of P4VP-*b*-PS in toluene is 66 mN m^{-1}, similar to the 68 mN m^{-1} for pure PS in Fig. 5b.

For the copolymers containing DO13, Fig. 7 shows isotherms shifted to larger areas in comparison with the pure copolymer,

Fig. 6. Surface pressure isotherms for the pure copolymer PS-*b*-P4VP in toluene (TOL) and chloroform (CHLO).

with collapse pressures around 50 mN m^{-1}. The extrapolated areas to zero pressure are 9.3 and 12.7 A^2 mol^{-1}, for systems with 25–40 wt.% DO13, respectively. Furthermore, the compressibility is lower than for the isotherms obtained with the DO13-containing copolymers dissolved in chloroform in Fig. 4, as indicated by the steeper curves in the liquid-condensed phase.

3.2. Photoinduced birefringence

In order to analyze the influence from film structure on the photoinduced birefringence, we investigated the optical behavior of LB, LS and spin-coated films. Optimized conditions for transferring the films from the air/water interface were obtained in a systematic study, based on which we chose surface pressures close to 30 mN m^{-1} for LB and LS transfer. This pressure was near (but below) the collapse region, and therefore the resulting films should be homogeneous and compact, which are desirable characteristics from the point of view of the optical properties.

3.2.1. Homopolymer P4VP(DO13)

Homogeneous LS and LB films up to 10 layers were transferred onto glass substrates from Langmuir films of P4VP(DO13), with 25 and 40 wt.% of azo chromophore, at 35 mN m^{-1}. Fig. 8 shows the
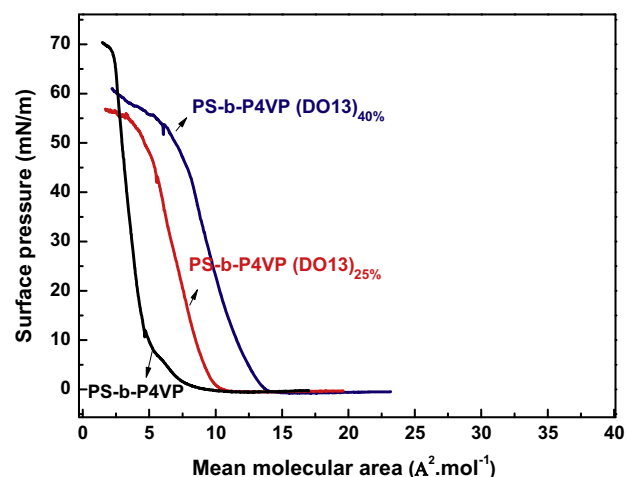

Fig. 7. Surface pressure isotherms for PS-*b*-P4VP and PS-*b*-P4VP(DO13) spread with toluene with 25 and 40 wt.% DO13.
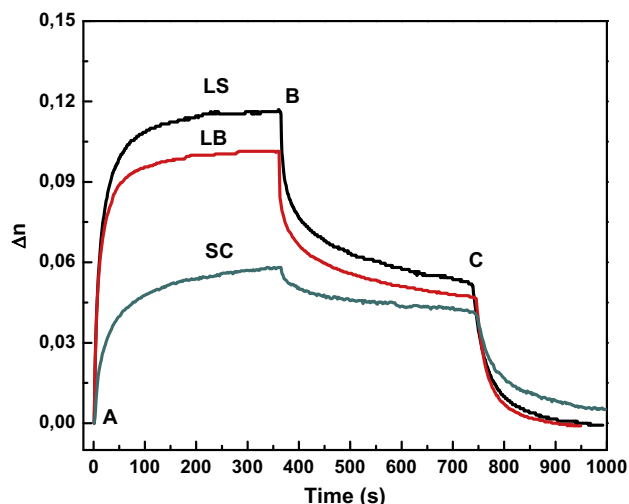
Fig. 8. Comparison of the optical behavior of LB, LS and SC films of P4VP(DO13) with 25 wt.% DO13.

Fig. 9. Typical writing and erasing curves for 20-layer LS films of PS-b-P4VP(DO13) with 25 and 40 wt.% DO13 (in chloroform).

optical storage curves for P4VP(DO13) films prepared using the different deposition techniques. At the beginning of the experiment, no light was transmitted through the analyzer as the azo chromophores were randomly oriented. The linearly polarized writing laser beam was turned on at (A), and the photoinduced birefringence rose sharply before approaching the saturation level. This is a consequence of trans–cis–trans photoisomerizations that led to the orientation of some *trans* molecules perpendicular to the polarization vector of the writing beam. When the excitation light was turned off at (B), the signal decreased owing to thermal relaxation of some azobenzene molecules until leveling off. To remove the remaining birefringence, circularly polarized light was turned on at point C, and the film returned to the isotropic state.

The optical storage curves in Fig. 8 indicate a faster writing process for LB and LS films, with the time required to reach 80% of the maximum birefringence ($t_{0,8}$) being 36 and 34 s, respectively. This time was ca. one third of the value required for the spin-coated films (105 s). Therefore, the ability of the chromophores to reorient in LB and LS films is higher than in SC films. In addition, the maximum birefringence (Δn) for 10-layer LB and LS films (Δn = 0.115 and 0.101, respectively) was almost double the value for the spin-coated film (Δn = 0.058). The enhanced birefringence for LB and LS films is consistent with data in the literature [7,23–25] and has been attributed to the ordered nature of nanostructured films built in a layer-by-layer fashion [23,26]. The residual birefringence, on the other hand, was higher for the SC film that retains 72% of the maximum signal after the writing laser was turned off, to be compared with 45% for LB and LS films. This was not expected because residual birefringence is generally higher for LB films [3,27,28]. However, a similar result was reported for an epoxy-amine system [25], where the lower residual birefringence for LB films was ascribed to the same factors that induce high chromophore mobility and lead to faster writing times and high birefringence values. According to this rationale, the chromophores would be amenable to reorient after the laser was turned off.

3.2.2. Block copolymer PS-b-P4VP(DO13) (in chloroform)

Fig. 9 shows typical writing and erasing curves for PS-b-P4VP(DO13) 20-layer LS films, obtained at a deposition pressure of 25 mN m^{-1}, for the two different percentages of azobenzene. The time required to reach 80% of maximum birefringence was 61 and 55 s for samples with 25 and 40 wt.% DO13, respectively, i.e. writing is faster with increasing dye concentration, as expected.
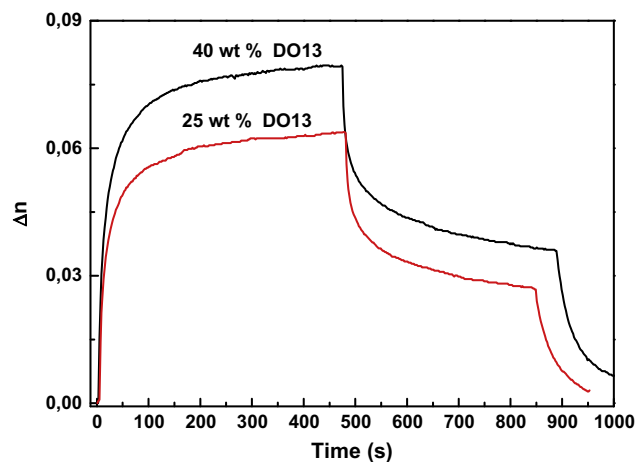
The maximum birefringence achieved was 0.064 for the sample with 25 wt.% DO13 and 0.079 for 40 wt.% DO13. Despite the high values of maximum birefringence, only 40% of the birefringence signal were retained after turning off the writing beam, similarly to the case of the homopolymers.

3.2.3. Block-copolymer PS-b-P4VP(DO13) (in toluene)

LS films with 20 layers were prepared at a deposition pressure of 30 mN m^{-1}, with the two different percentages of azobenzene. Optical storage curves for these films are shown in Fig. 10, again featuring a shorter writing time ($t_{0,8}$) for films with higher percentages of DO13.

The solvent for spreading the Langmuir film also affected the writing time and maximum birefringence, as indicated in Fig. 11 for 20-layer LS films with 40 wt.% DO13. The film obtained from a toluene solution displayed a writing time that was less than half the value for the film prepared with chloroform, in addition to a higher maximum birefringence. The latter was 0.105 and 0.079 for the LS films prepared in toluene and chloroform, respectively. This improved behavior could be attributed to the ordered morphology developed in toluene that makes a confinement effect over the azobenzene, avoiding randomization and increasing anisotropy.
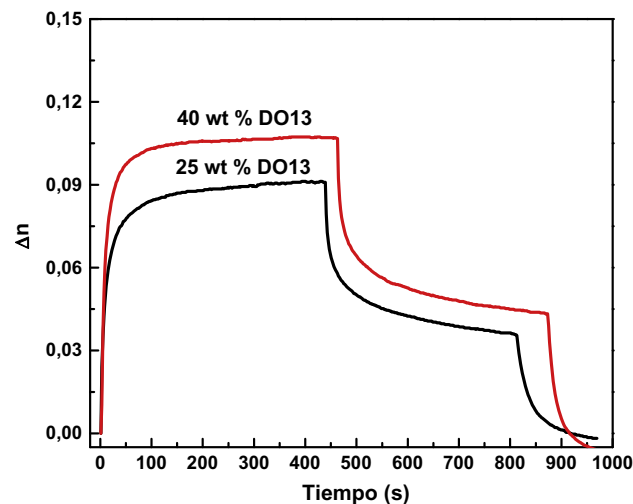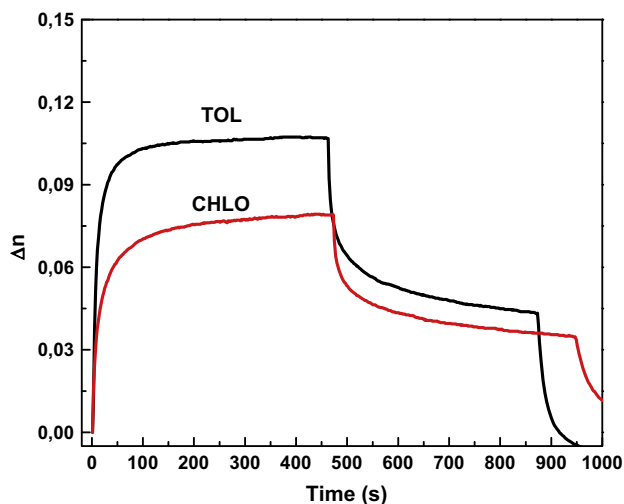

Fig. 10. Typical writing and erasing curves for 20-layer LS films of PS-b-P4VP(DO13) with 25 and 40 wt.% DO13 (in toluene).
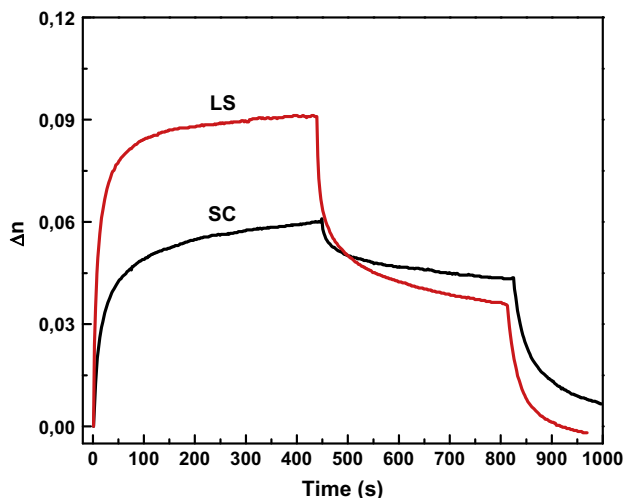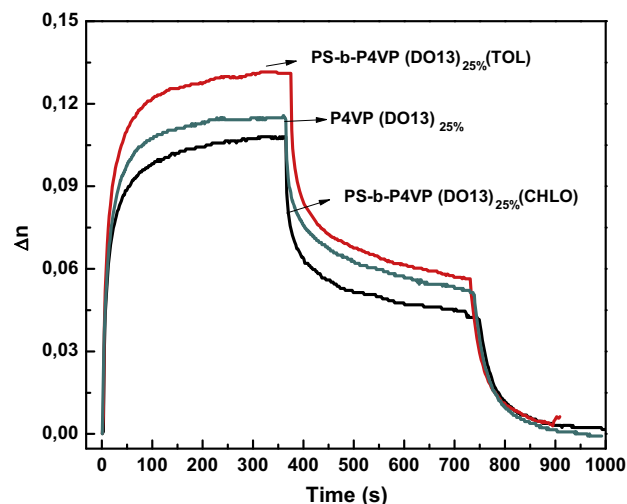
Fig. 11. Comparison of the optical behavior of 20-layer LS films of PS-*b*-P4VP(DO13) with 40 wt.% DO13 in toluene and chloroform.

Fig. 13. Comparison of the optical behavior of 10-layer LB films obtained for the copolymer (in toluene and chloroform) and the homopolymer P4VP with the same percentage of azobenzene.

Fig. 12 shows the curves for the system with 25 wt.% DO13 in toluene using different film preparation techniques (LS and SC). Again, the increase in the signal was faster for LS films, with $t_{0,8}$ of 33 s, close to one third of the 90 s for the SC film. Furthermore, the maximum birefringence was 0.09 and 0.06 for the 20-layer LS film and the SC film, respectively.

Fig. 13 compares the 10-layer LB films obtained with a deposition pressure of 30 mN m^{-1} for all the systems with 25 wt.% DO13 in different solvents. Again, we found a similar behavior to that obtained for the LS films. When comparing the results with those of the homopolymer higher values of birefringence were obtained for copolymer films in toluene. All of these improvements in the optical properties could be attributed to the confinement effect of the copolymer micelles over the azobenzene, which avoid randomization and leads to increased anisotropy. One possible cause of this amplification in the birefringence values may be attributed to cooperative movements of different groups. It is possible that when movement is induced in azobenzene groups, the intrinsic thermodynamic tendency to organize in ordered phases forces other polymer chain rigid groups to move together.

One should stress that the response times were much longer than expected for LS and LB films. This behavior could be attributed to the chemical nature of the bisazobenzene. Natansohn and Rochon reported [29] that the writing speed is related to the polarity of azobenzene, with shorter times being obtained for increasingly polar azobenzene groups. In our case, the bisazobenzene is not too polar and this could be the cause of the longer times required to achieve the maximum birefringence. Another possible explanation is that bisazobenzene molecules may only be photoaligned if the two azo groups are photoisomerized simultaneously, thus hampering the photoalignment process [30].

4. Conclusions

Nanostructured Langmuir–Blodgett (LB) and Langmuir–Schaefer (LS) films were obtained from PS-*b*-P4VP(DO13) copolymers, whose optically induced birefringence was considerably higher than for cast films of the same copolymers. Marked differences were noted upon using two different solvents in preparing the Langmuir films. For toluene, which is a selective solvent for one of the blocks of the copolymer, a higher film-forming ability was observed in the surface pressure isotherms in comparison to the isotherms for the copolymers dissolved in the non-selective chloroform. This had a pronounced effect on the optical storage capability of the LS and LB films, with a higher photoinduced birefringence for the films prepared with toluene. Furthermore, the writing times were also shorter for the LB and LS films fabricated from toluene solutions. The enhanced properties with toluene are ascribed to the formation of micelles consisting of a P4VP core and a PS corona [17], owing to a cooperative effect arising from the confinement effect over azo chromophores.

Fig. 12. Typical writing and erasing curves for PS-*b*-P4VP(DO13) with 25 wt.% DO13 using different film preparation techniques (LS and SC).

References

[1] T. Mori, K. Sakakibara, H. Endo, M. Akada, K. Okamoto, A. Shundo, M.V. Lee, Q.M. Ji, T. Fujisawa, K. Oka, M. Matsumoto, H. Sakai, M. Abe, J.P. Hill, Langmuir 29 (24) (2013) 7239.

[2] M. Ramanathan, L.K. Shrestha, T. Mori, Q. Ji, J.P. Hill, K. Ariga, Phys. Chem. Phys. 15 (2013) 10580.

[3] M. Haro, B. Giner, I. Gascon, F.M. Royo, M.C. López, Macromolecules 40 (2007) 2058.

[4] A. Ulman, An Introduction to Ultrathin Organic Films: From Langmuir–Blodgett to Self-Assembly, Academic Press, San Diego, 1991.

[5] O.N. Oliveira Jr., M. Raposo, A. Dhanabalan, Langmuir–Blodgett (LB) and Self-Assembled Polymeric Films, Academic Press, New York, 2001.

[6] T. Seki, T. Fukuchi, T. Kobayashi, K. Ichimura, Bull. Chem. Soc. Jpn. 76 (11) (2003) 2217.

[7] O.N. Oliveira Jr., D.S. dos Santos Jr., D.T. Balogh, V. Zucolotto, C.R. Mendonca, Adv. Colloid Interface Sci. 116 (2005) 179.

[8] A. Dhanabalan, C.R. Mendonca, D.T. Balogh, L. Misoguti, C.J.L. Constantino, J.A. Giacometti, Macromolecules 32 (1999) 5277.

[9] P. Dynarowicz-Latka, A. Dhanabalan, O.N. Oliveira Jr., Adv. Colloid Interface Sci. 91 (2001) 221.

[10] F. Pavinatto, J.Y. Barletta, R.C. Sanfelice, M.R. Cardoso, D.T. Balogh, C.R. Mendonça, O.N. Oliveira Jr., Polymer 50 (2009) 491.

[11] M. Matsumoto, S. Terrettaz, H. Tachibana, Adv. Colloid Interface Sci. 87 (2009) 147.

[12] L. Zhang, A. Eisenberg, Macromolecules 32 (1999) 2239.

[13] X. Wang, X. Ma, D. Zang, Soft Matter 9 (2013) 443.

[14] J.Y. Park, R.C. Advincula, Soft Matter 7 (2011) 9829.

[15] E.W. Price, S. Harirchian-Saei, M.G. Moffitt, Strands, Langmuir 27 (4) (2010) 1364.

[16] G. Wen, B. Chung, T. Chang, Polymer 47 (2006) 8575.

[17] L.M. Sáiz, P.A. Oyanguren, M.J. Galante, I.A. Zucchi, Nanotechnology 25 (2014) 065601.

[18] L.M. Sáiz, A.B. Orofino, M.M. Ruzzo, G.F. Arenas, P.A. Oyanguren, M.J. Galante, Polym. Int. 60 (2011) 1053.

[19] C. Price, I. Goodman (Eds.), Developments in Block Copolymers, vol. 1, Applied Science Publishers, London, 1982, p. 39.

[20] J. Selb, Y. Gallot, Ionic block copolymers, in: I. Goodman (Ed.), Developments in Block Copolymers, vol. 2, Applied Science Publishers, London, 1985, p. 27.

[21] A. Halperin, M. Tirrell, T.P. Lodge, Adv. Polym. Sci. 100 (1992) 31.

[22] Z. Tuzar, P. Kratochvil, Micelles of block and graft copolymers in solution, in: E. Matijevic (Ed.), Surface and Colloid Science, vol. 15, Plenum Press, New York, 1993, p. 1.

[23] M. Ferreira, C.J.L. Constantino, C.A. Olivati, D.T. Balogh, R.F. Aroca, R.M. Faria, O.N. Oliveira Jr., Polymer 46 (2005) 5140.

[24] R. Fernández, I. Mondragon, R.C. Sanfelice, F.J. Pavinatto, O.N. Oliveira Jr., P.A. Oyanguren, M.J. Galante, Mater. Sci. Eng., C 33 (2013) 1403.

[25] C.A. Olivati, M. Ferreira, A.J.F. Carvalho, D.T. Balogh, O.N. Oliveira Jr., H.V. Segern, Chem. Phys. Lett. 408 (2005) 31.

[26] L.F. Ceridório, D.T. Balogh, L. Caseli, M.R. Cardoso, T. Viitala, C.R. Mendonça, O.N. Oliveira Jr., J. Colloid Interface Sci. 346 (2010) 87.

[27] H. Tachinaba, R. Azumi, M. Tanaka, S. Matsumoto, H. Tako, M. Sakai, Y. Abe, N. Kondo, M. Yoshino, Thin Solid Films 284 (1996) 73.

[28] C.R. Mendonça, A. Dhanabalan, D.T. Balogh, C.J.L. Misoguti, D.S. dos Santos Jr., M.A. Pereira-da-Silva, S.C. Giacometti, S.C. Zilio, O.N. Oliveira Jr., Macromolecules 32 (1999) 1493.

[29] A. Natansohn, P. Rochon, Chem. Rev. 102 (2002) 4139.

[30] C.R. Mendonça, C.J.L. Misoguti, A.A. Andrade, S.B. Yamaki, V.D. Dias, T.D.Z. Atvars, O.N. Oliveira Jr., Opt. Mater. 30 (2007) 216.